

Regioselective  $\beta$ -Metalation of *meso*-Phosphanylporphyrins. Structure and Optical Properties of Porphyrin Dimers Linked by Peripherally Fused PhosphametallacyclesYoshihiro Matano,<sup>\*,†</sup> Kazuaki Matsumoto,<sup>†</sup> Yoshihide Nakao,<sup>†</sup> Hidemitsu Uno,<sup>†</sup> Shigeyoshi Sakaki,<sup>†</sup> and Hiroshi Imahori<sup>†,§</sup>

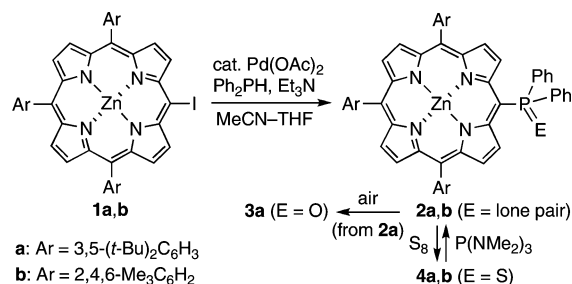
Department of Molecular Engineering, Graduate School of Engineering, Kyoto University, Nishikyo-ku, Kyoto 615-8510, Japan, Integrated Center for Sciences, Ehime University, Matsuyama 790-8577, Japan, and Institute for Integrated Cell-Material Sciences, Kyoto University, Nishikyo-ku, Kyoto 615-8510, Japan

Received November 22, 2007; E-mail: matano@scl.kyoto-u.ac.jp

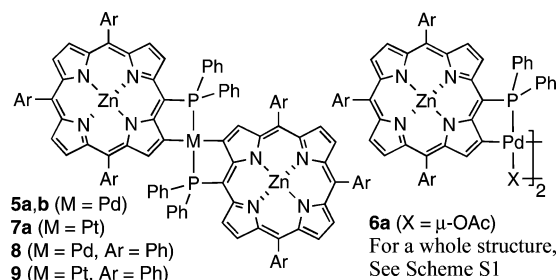
Peripherally metalated porphyrins bearing a carbon–metal  $\sigma$ -bond play a crucial role in transition-metal-catalyzed functionalization of porphyrin rings.<sup>1</sup> This class of compounds should also provide valuable information on electronic communication between the porphyrin  $\pi$ -system and the metal d orbitals attached at the periphery. Arnold and co-workers investigated the structures and fundamental properties of *meso*- $\eta^1$ -palladio- and platinoporphyryns, which were prepared by oxidative addition of the corresponding zerovalent metals to C–Br bonds of *meso*-bromoporphyrins.<sup>2</sup> Recently, Osuka, Shinokubo, and co-workers synthesized the pincer-type *meso*- $\eta^1$ -palladioporphyryns via *meso*-C–H activation directed by two neighboring 2-pyridyl groups.<sup>3</sup> However, the number of structurally characterized examples, especially those containing a  $\beta$ -C–M bond,<sup>4,5</sup> is still limited. Here we report the first examples of  $\beta$ - $\eta^1$ -palladio- and platinoporphyryns, which are formed by regioselective metalation at the  $\beta$  carbon of *meso*-phosphanylporphyrins.<sup>6</sup> Most importantly, the coplanar porphyrin dimers linked by peripherally fused phosphametallacycles have been found to exhibit characteristic optical and electrochemical properties derived from the  $p_\pi$ – $d_\pi$  orbital interaction.

The Pd-catalyzed C–P cross-coupling reaction of *meso*-iodoporphyryns **1a,b**<sup>1c,e</sup> with diphenylphosphane in MeCN–THF produced the corresponding *meso*-phosphanylporphyrins **2a,b** as air-sensitive substances (Scheme 1). For instance, **2a** was oxidized rapidly in air to *meso*-phosphorylporphyrin **3a**.<sup>7</sup> Due to difficulty of isolating **2a,b** at this stage, the crude reaction mixtures were subsequently treated with elemental sulfur, affording *meso*-thiophosphorylporphyrins **4a,b** as air-stable solids in 87–92% yields based on **1a,b**. Desulfurization of **4a,b** with excess P(NMe<sub>2</sub>)<sub>3</sub> in refluxing toluene reproduced **2a,b** quantitatively. Remarkably, this two-step protocol enabled us to isolate pure **2a,b** in 90–95% isolated yields (based on **4a,b**) by simple reprecipitation under inert atmosphere.<sup>8</sup>

Treatment of **2a,b** with palladium(II) and platinum(II) salts yielded novel classes of porphyrin dimers **5**–**7**, which contain two phosphametallacycle linkages as depicted in Figure 1 and Scheme S1 (Supporting Information). The complexation of **2a** with 0.5 equiv of Pd(OAc)<sub>2</sub> in toluene afforded Pd-mononuclear complex **5a** and bis- $\mu$ -acetato-bridged Pd-dinuclear complex **6a** in 55% and 23% yield, respectively (Table 1, entry 1). When **2a** was slowly added to a toluene solution of 1 equiv of Pd(OAc)<sub>2</sub>, **6a** was formed predominantly in 73% yield (entry 2). By contrast, **2b** reacted with 0.5 equiv of Pd(OAc)<sub>2</sub> to produce Pd-mononuclear complex **5b** exclusively (entry 3). The complexation of **2a** with 0.5 equiv of PtCl<sub>2</sub>(cod) (cod = 1,5-cyclooctadiene) in the presence of Et<sub>3</sub>N gave

**Scheme 1.** Synthesis and Reactions of *meso*-Phosphanylporphyrins**Table 1.** Complexation of **2a,b** with Pd(II) and Pt(II) Salts

entry	2	MX <sub>2</sub> ·L/solvent	2/MX <sub>2</sub>	product (yield <sup>a</sup> )
1	<b>2a</b>	Pd(OAc) <sub>2</sub> /toluene	1/0.5	<b>5a</b> (55%), <b>6a</b> (23%)
2	<b>2a</b>	Pd(OAc) <sub>2</sub> /toluene	1/1	<b>5a</b> (trace), <b>6a</b> (73%)
3	<b>2b</b>	Pd(OAc) <sub>2</sub> /toluene	1/0.5	<b>5b</b> (70%)
4 <sup>b</sup>	<b>2a</b>	PtCl <sub>2</sub> (cod)/CH <sub>2</sub> Cl <sub>2</sub>	1/0.5	<b>7a</b> (62%)

<sup>a</sup> Isolated yield based on **2a,b**. <sup>b</sup> Et<sub>3</sub>N was added.**Figure 1.** Structures of  $\beta$ - $\eta^1$ -palladio- and platinoporphyryns **5**–**9**.

Pt-mononuclear complex **7a** in 62% yield (entry 4). All the products were fully characterized by MS and NMR spectroscopies. In the MS spectra, intense molecular ion peaks were detected. The <sup>31</sup>P NMR spectra displayed single peaks at  $\delta$  46.7–51.1,<sup>8</sup> indicating that two phosphorus atoms coordinate to the palladium or platinum center equivalently. The <sup>31</sup>P–<sup>195</sup>Pt coupling constant of 2834 Hz observed for **7a** suggests that the two phosphine ligands are coordinated in a trans geometry. The appearance of seven kinds of peripheral  $\beta$  protons (each 2H) in the <sup>1</sup>H NMR spectra of **5**–**7** reveals that one of the  $\beta$ -H atoms of the porphyrin ring is replaced by the Pd(II) or Pt(II) salt through the complexation (Figures S24–S27, Supporting Information). It is likely that the *meso*-phosphanyl group directs the P-ligated metal center to activate the neighboring  $\beta$ -C–H bond regioselectively.

The structure of **5b** was unambiguously elucidated by X-ray crystallography.<sup>9</sup> As shown in Figures 2 and S1 (Supporting

<sup>†</sup> Graduate School of Engineering, Kyoto University.<sup>‡</sup> Ehime University.<sup>§</sup> Institute for Integrated Cell-Material Sciences, Kyoto University.

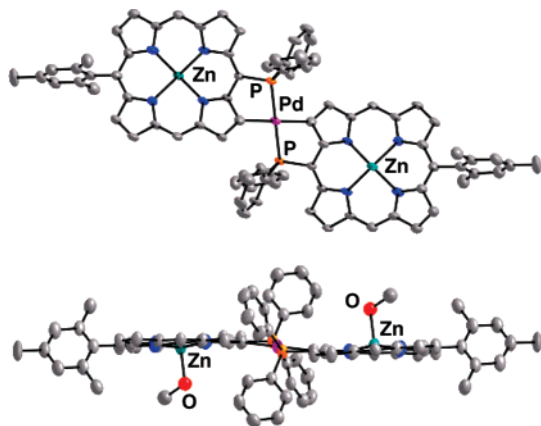


**Figure 2.** Top view (upper) and side view (lower) of **5b**. Hydrogen atoms, 10,20-*meso*-aryl groups, solvents, and MeOH (top view) are omitted for clarity: Pd–C $_{\beta}$ , 2.046(4) Å; Pd–P, 2.2904(14) Å; C $_{\beta}$ –Pd–P, 81.84(11) $^{\circ}$  and 98.16(11) $^{\circ}$ ; Pd–P–C $_{meso}$ , 104.85(13) $^{\circ}$ .

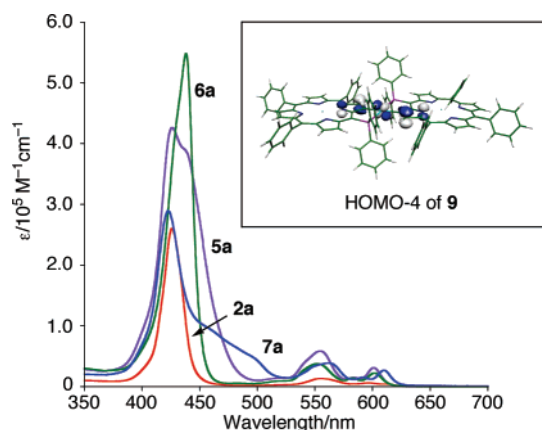


**Figure 3.** UV-vis absorption spectra of **2a** (red), **5a** (purple), **6a** (green), and **7a** (blue) in toluene. The inset shows HOMO-4 of **9**.

Information), the Pd center in the phosphapalladacycles adopts a distorted square planar geometry ( $\Sigma_{C-Pd-P} = 360^{\circ}$ ) with  $C_i$  symmetry. As a consequence, two porphyrin rings are almost on the same plane with a Zn–Zn distance of 12.1 Å.<sup>10</sup> The Pd–C bond length [2.046(4) Å] of **5b** is comparable to the reported value [2.05(2) Å] of Arnold's *meso*- $\eta^1$ -palladioporphyrin<sup>2a</sup> and longer than those [1.969(6)–1.977(7) Å] of Osuka's pincer-type *meso*- $\eta^1$ -palladioporphyrins.<sup>3</sup>

The UV-vis absorption spectra of phosphanylporphyrin **2a** and the Pd-dinuclear complex **6a** displayed relatively narrow Soret bands at  $\lambda_{max}$  426 and 438 nm, respectively (Figures 3 and S2, Supporting Information). In sharp contrast, the Pd- and Pt-mononuclear complexes **5a** and **7a** showed rather broad absorptions at the Soret-band regions ( $\lambda_{max} = 426$  and 422 nm). To gain a deep insight into the character of these transitions, we performed time-dependent density functional theory (TD-DFT) calculations of their model complexes **8** and **9** and 5,10,15,20-tetraphenylporphyrinatozinc(II) (TPPZn) (Figures S3–S14 and Tables S1–S4, Supporting Information). Notably, the excitations from HOMO-4 largely contribute to Soret bands of **8** and **9**, which are split or broadened as compared to that calculated for TPPZn, although the calculated excitation energies are somewhat larger than the observed values.<sup>11</sup> As visualized in Figures S5–S8 (Supporting Information) and 3 (inset), the HOMO-4 in **8** and **9** involves antibonding character between the pyrrolic  $p_{\pi}$  orbitals and the metal  $d_{\pi}$  orbital, which implies possible electronic communication between the coplanar porphyrin  $\pi$  systems through the peripheral  $\beta$ -C–M bonds. Indeed,

cyclic voltammograms of **5a** and **7a** displayed appreciably broadened or split cathodic and anodic waves for their electrochemical oxidation processes (Figure S19, Supporting Information),<sup>12</sup> suggesting that the  $\pi$ -radical cations delocalize over the metal-linked two porphyrin rings. The relatively large splitting potential ( $\Delta E_{ox} = 0.06$  V) observed for **7a** indicates that the delocalization between the Pt-linked porphyrin  $\pi$  systems occurs more efficiently than that between the Pd-linked  $\pi$  systems.

In summary, we have successfully applied the phosphane-directed regioselective  $\beta$ -C–H activation by Pd(II) and Pt(II) salts to the synthesis of new classes of porphyrin dimers linked by the peripherally fused phosphametallacycles. The present results demonstrate that the  $p_{\pi}$ – $d_{\pi}$  orbital interaction at the peripheral  $\beta$ -carbon–metal bond potentially affects the optical and electrochemical properties of the metal-linked coplanar porphyrin  $\pi$  systems.

**Acknowledgment.** This work was partially supported by Grants-in-Aid (No. 17350018 and No. 461) from the Ministry of Education, Culture, Sports, Science and Technology of Japan. We thank Dr. Motoo Shiro for X-ray crystallography.

**Supporting Information Available:** Experimental details, CIF file for **5b**, and DFT computational results. This material is available free of charge via the Internet at <http://pubs.acs.org>.

## References

- (1) For example, see: (a) DiMaggio, S. G.; Lin, V. S.-Y.; Therien, M. J. *J. Am. Chem. Soc.* **1993**, *115*, 2513–2515. (b) Lin, V. S.-Y.; DiMaggio, S. G.; Therien, M. J. *Science* **1994**, *264*, 1105–1111. (c) Shultz, D. A.; Gwaltney, K. P.; Lee, H. J. *J. Org. Chem.* **1998**, *63*, 769–774. (d) Shanmugathasan, S.; Johnson, C. K.; Edwards, C.; Matthews, E. K.; Dolphin, D.; Boyle, R. W. *J. Porphyrins Phthalocyanines* **2000**, *4*, 228–232. (e) Odobel, F.; Suzenet, F.; Blart, E.; Quintard, J.-P. *Org. Lett.* **2000**, *2*, 131–133. (f) Hata, H.; Shinokubo, H.; Osuka, A. *J. Am. Chem. Soc.* **2005**, *127*, 8264–8265.
- (2) (a) Arnold, D. P.; Sakata, Y.; Sugiura, K.; Worthington, E. I. *Chem. Commun.* **1998**, 2331–2332. (b) Arnold, D. P.; Healy, P. C.; Hodgson, M. J.; Williams, M. L. *J. Organomet. Chem.* **2000**, *607*, 41–50. (c) Hodgson, M. J.; Healy, P. C.; Williams, M. L.; Arnold, D. P. *J. Chem. Soc., Dalton Trans.* **2002**, 4497–4504. (d) Hartnell, R. D.; Edwards, A. J.; Arnold, D. P. *J. Porphyrins Phthalocyanines* **2002**, *6*, 695–707. (e) Hartnell, R. D.; Arnold, D. P. *Organometallics* **2004**, *23*, 391–399. (f) Hartnell, R. D.; Arnold, D. P. *Eur. J. Inorg. Chem.* **2004**, 1262–1269.
- (3) Yamaguchi, S.; Katoh, T.; Shinokubo, H.; Osuka, A. *J. Am. Chem. Soc.* **2007**, *129*, 6392–6393.
- (4) Smith, K. M.; Langry, K. C.; Minnetian, O. M. *J. Org. Chem.* **1984**, *49*, 4602–4609.
- (5) Quite recently, Sugiura, Arnold, and co-workers reported the regioselective synthesis and crystal structure of  $\beta$ -HgCl-substituted porphyrins. See: Sugiura, K.-i.; Kato, A.; Iwasaki, K.; Miyasaka, H.; Yamashita, M.; Hino, S.; Arnold, D. P. *Chem. Commun.* **2007**, 2046–2047.
- (6) Matano, Y.; Matsumoto, K.; Terasaka, Y.; Hotta, H.; Araki, Y.; Ito, O.; Shiro, M.; Sasasmori, T.; Tokitoh, N.; Imahori, H. *Chem. Eur. J.* **2007**, *13*, 891–901.
- (7) Arnold suggested the formation of a *meso*-phosphanylporphyrin as the intermediate in their synthesis of *meso*-phosphorylporphyrins. See: (a) Atefi, F.; Locos, O. B.; Senge, M. O.; Arnold, D. P. *J. Porphyrins Phthalocyanines* **2006**, *10*, 176–185. (b) Atefi, F.; McMurtrie, J. C.; Turner, P.; Duriska, M.; Arnold, D. P. *Inorg. Chem.* **2006**, *45*, 6479–6489.
- (8)  $\delta_P$  (162 MHz; CDCl $_3$  or CD $_2$ Cl $_2$ ) of **2a**, **2b**, **5a**, **5b**, **6a**, and **7a** are –5.4, –6.0, 51.1, 48.6, 50.5, and 46.7 ( $^1J_P$ –Pt = 2834 Hz), respectively.
- (9) C $_{140}$ H $_{134}$ N $_8$ O $_4$ P $_2$ PdZn $_2$ ,  $P1$ ,  $a = 11.030(5)$  Å,  $b = 16.207(8)$  Å,  $c = 16.613(8)$  Å,  $\alpha = 97.695(8)^{\circ}$ ,  $\beta = 91.885(8)^{\circ}$ ,  $\gamma = 98.247(9)^{\circ}$ ,  $V = 2909(2)$  Å $^3$ ,  $Z = 1$ ,  $D_c = 1.308$  g cm $^{-3}$ , 13199 obsd, 764 variables,  $R_w = 0.1690$ ,  $R = 0.0691$  ( $I > 2.00\sigma(I)$ ), GOF = 1.064. Although the quality of crystallographic data is not at the publishable level, a similar planar structure of **7a** was confirmed by X-ray diffraction analysis.
- (10) The zinc atom is deviated from the 24-atom mean plane (0.32 Å) due to the coordination by the methanol-oxygen.
- (11) The calculated wavelengths of Soret bands are red-shifted when solvation effects are incorporated. In a Zn analog of **8**, the splitting of Soret band becomes much smaller, indicating that the  $p_{\pi}$ – $d_{\pi}$  orbital interaction between porphyrin and bridging Pd atom is important to lead to a broad Soret band of **8**. For details, see the Supporting Information.
- (12)  $E_{ox}$  and  $E_{red}$  (vs Fc/Fc $^{+}$ ; in CH $_2$ Cl $_2$  with 0.1 M  $n$ Bu $_4$ N $^{+}$ PF $_6^{-}$ ; Ag/Ag $^{+}$  [0.01 M AgNO $_3$  (MeCN)]): +0.35/+0.60 V and –1.82 V for **5a**; +0.42/+0.67 V and –1.71 V for **6a**; +0.31/+0.37/+0.57 V and –1.83 V for **7a**.

JA710542E